Noncollective nucleon pairs in even-even $^{124-128}$Sn

B. C. He (何秉承),[1] H. T. Xue (薛怀通),[1] Lei Li (李磊),[1,*] Y. A. Luo (罗延安),[1,†] Y. Zhang (张宇),[2,‡] F. Pan (潘峰),[2,3] and J. P. Draayer[3]

[1]*School of Physics, Nankai University, Tianjin, 300071, People's Republic of China*
[2]*Department of Physics, Liaoning Normal University, Dalian 116029, People's Republic of China*
[3]*Department of Physics and Astronomy, Louisiana State University, Baton Rouge, Louisiana 70803, USA*

(Received 1 October 2019; revised manuscript received 22 November 2019; published 31 January 2020)

The effects of possible noncollective pairs in even-even $^{124-128}$Sn are studied in the nucleon-pair shell model, in which a few noncollective neutron pairs originating from the alignment of two neutrons in the $\nu h_{11/2}$ orbit are considered. From the low-lying-level energies, $B(E2)$ ratios, and excited states obtained from the model, it is shown that the yrast band structure can be explained as the evolution from vibrational to rotational type as a function of spin. The mechanism of the yrast band can be explained as band crossing between the ground-state band and the S band constructed from the neutron alignment in the $\nu h_{11/2}$ orbit. The noncollective configurations may be crucial for describing the yrast states in even-even ^{124,126,128}Sn in the SD-pair shell model.

DOI: 10.1103/PhysRevC.101.014324

I. INTRODUCTION

Based on the generalized Wick theorem for coupled operators [1,2], the nucleon-pair shell model (NPSM) has been proposed [3], in which collective nucleon pairs with various angular momenta serve as basic building blocks [4]. One advantage of the NPSM is that the Hamiltonian can be diagonalized in a fermion-pair subspace directly, and it also allows for various truncation schemes ranging from an S-pair subspace up to the full paired subspace. However, because the CPU time needed for the computation increases dramatically with the increasing of the number of pairs and orbitals, guided by the success of the interacting boson model (IBM), one normally truncates the model space for medium- and heavy-mass nuclei to a collective S- and D-pair subspace, for which it is called the SD-pair shell model (SDPSM) [4,5]. The NPSM has also been generalized to the case with isospin degrees of freedom [6].

Our previous work shows that with only one kind of S-pair and D-pair considered, the SDPSM can reproduce the main properties of the $U(5)$, the $SU(3)$, the $O(6)$, and the $SU^*(3)$ limiting cases of the IBM, which correspond to the vibrational, rotational, γ-unstable, and triaxial cases described by the collective model, respectively [7,8]. The quantum phase transitional patterns and the associated critical-point symmetries can also be well reproduced in the SDPSM [9,10].

In Refs. [11,12], in order to describe the backbending phenomena in ^{132}Ba and ^{132,134,136}Ce, one noncollective pair occupying the $h_{11/2}$ orbit was considered in the SDPSM, and it was found that two neutrons in the $h_{11/2}$ orbit coupled to angular momentum $I = 10$ noncollective pair may play an important role in the first backbending for those nuclei. The $B(E2)$ feature of a sudden drop in the backbending region can also be well simulated in those works. These results demonstrate that subspace spanned by the truncated collective SD pairs and one noncollective pair with $I = 10$ seems an effective and minimal shell-model subspace to elucidate the phenomena. In this work, effects of the number of noncollective pairs and their contribution to excited states described in the SDPSM will be studied.

It is known that, for heavy tin isotopes, the 6^+, 8^+, and 10^+ states in the yrast band are almost degenerate and noncollective. But the 2^+, 4^+, and the states with $I > 10$ are not degenerate and collective. Because of the special structure of the spectra, the Sn isotopes have been studied extensively [13–27]. Reference [28] shows that the excited states of heavy Sn for mass number A $\geqslant$ 120 are expected to be described by considering valence neutrons moving in a spherical well, while the excited levels above 3 MeV are ascribed to several broken pairs of valence neutrons occupying the $\nu h_{11/2}$ orbit. Therefore, in order to study the effect of noncollective pairs, the yrast band of ^{124,126,128}Sn will be considered as examples with noncollective pairs in the SDPSM, in which at most two noncollective pairs with $I = 0$, 2, 4, 6, 8, and 10 occupying the $h_{11/2}$ orbit are possible.

II. THE MODEL

In the SDPSM, the collective S and D pairs are defined as

$$\begin{aligned} A^{r\dagger}_{\mu} &= \sum_{ab} y(abr) A^{r\dagger}_{\mu}(ab), \quad r = 0,\ 2, \\ A^{r\dagger}_{\mu}(ab) &= (C^{\dagger}_{a} \times C^{\dagger}_{b})^{r}_{\mu}, \\ y(abr) &= -\theta(abr) y(bar), \\ \theta(abr) &= (-1)^{a+b+r}, \end{aligned} \tag{1}$$

*lilei@nankai.edu.cn
†luoya@nankai.edu.cn
‡dlzhangyu_physics@163.com

where $A_\mu^{r\dagger}(ab)$ denotes noncollective pairs with angular momentum r, $y(abr)$ is the structure coefficient, and $C_a^\dagger$ is the creation operator for a single nucleon with angular momentum j_a. As an approximation, in this work the S-pair structure coefficient is chosen to be $y(aa0) = \hat{j}_a \frac{\nu_a}{\mu_a}$, where ν_a and μ_a are occupied and empty amplitudes obtained by solving the BCS equation, while the D-pair structure coefficients are obtained from the commutator

$$A_\mu^{2\dagger} = D_\mu^\dagger = \tfrac{1}{2}\left[Q_\mu^{(2)}, S^\dagger\right], \tag{2}$$

where $S^\dagger = A_\mu^{0\dagger}$, and $Q^{(2)}$ is quadrupole operator with

$$\begin{aligned} Q_\mu^{(2)} &= \sum_{cd} q(cd2) P_\mu^2(cd), \\ q(cd2) &= (-1)^{j_c - \frac{1}{2}} \frac{\hat{j}_c \hat{j}_d}{\sqrt{20\pi}} C^{20}_{j_c \frac{1}{2}, j_d - \frac{1}{2}} \Delta_{cd2} \langle N l_c | r^2 | N l_d \rangle, \\ \Delta_{cd2} &= \frac{1}{2}[1 + (-1)^{l_c + l_d + 2}], \\ P_\mu^2(cd) &= (C_c^\dagger \times \tilde{C}_d)_\mu^2, \\ \hat{j}_a &= \sqrt{2 j_a + 1}. \end{aligned} \tag{3}$$

Here N is the principal quantum number of the spherical harmonic oscillator with the energy $(N + \frac{3}{2})\hbar\omega_0$, while l_c and l_d are orbital angular-momentum quantum number of the single particle at level c and d, respectively, $C^{20}_{j_c \frac{1}{2}, j_d - \frac{1}{2}}$ is the Clebsch-Gordan (CG) coefficient, and the time-reversal operator $\tilde{C}_a$ is denoted as $\tilde{C}_{j_a m_a} = (-)^{j_a - m_a} C_{j_a - m_a}$. The matrix element $\langle N l_c | r^2 | N l_d \rangle$ is given by

$$\langle N l_c | r^2 | N l_d \rangle = \begin{cases} \left(N + \frac{3}{2}\right) r_0^2, & l_c = l_d \\ \varphi \sqrt{(N + l_d + 2 \pm 1)(N - l_d + 1 \mp 1)}\, r_0^2, & l_c = l_d \pm 2, \end{cases}$$

where the phase factor φ can be taken as ± 1, $r_0^2 = \frac{\hbar}{M_N \omega_0} = 1.012 A^{\frac{1}{3}}$ fm^2, M_N is the mass of a nucleon, and ω_0 is the frequency of the harmonic oscillator.

As in Refs. [11,12], to study the effects of the noncollective pairs in ^{124,126,128}Sn, we consider at most two noncollective pairs occupying the $\nu h_{11/2}$ orbit,

$$A_\mu^{r\dagger}\left(\frac{11}{2}^- \frac{11}{2}^-\right) = (C_{11/2}^\dagger \times C_{11/2}^\dagger)_\mu^r, \tag{4}$$

where the angular momentum r of the noncollective pair can be taken as 0, 2, 4, 6, 8, or 10.

The creation operator for N pairs with angular momenta $r_1, \ldots, r_N$ coupled successively to the total angular momentum J_N and with J_i as the angular momentum for the first i pairs is designated by

$$\begin{aligned} A_{M_N}^{J_N\dagger}(r_i, J_i) &= A_{M_N}^{J_N\dagger} \\ &= (\cdots((A^{r_1\dagger} \times A^{r_2\dagger})^{J_2} \times A^{r_3\dagger})^{J_3} \times \cdots \times A^{r_N\dagger})_{M_N}^{J_N} \\ &\equiv A(r_1 r_2 \cdots r_N; J_1 J_2 \cdots J_N)^\dagger, \end{aligned} \tag{5}$$

in which the pairs can be collective or noncollective.

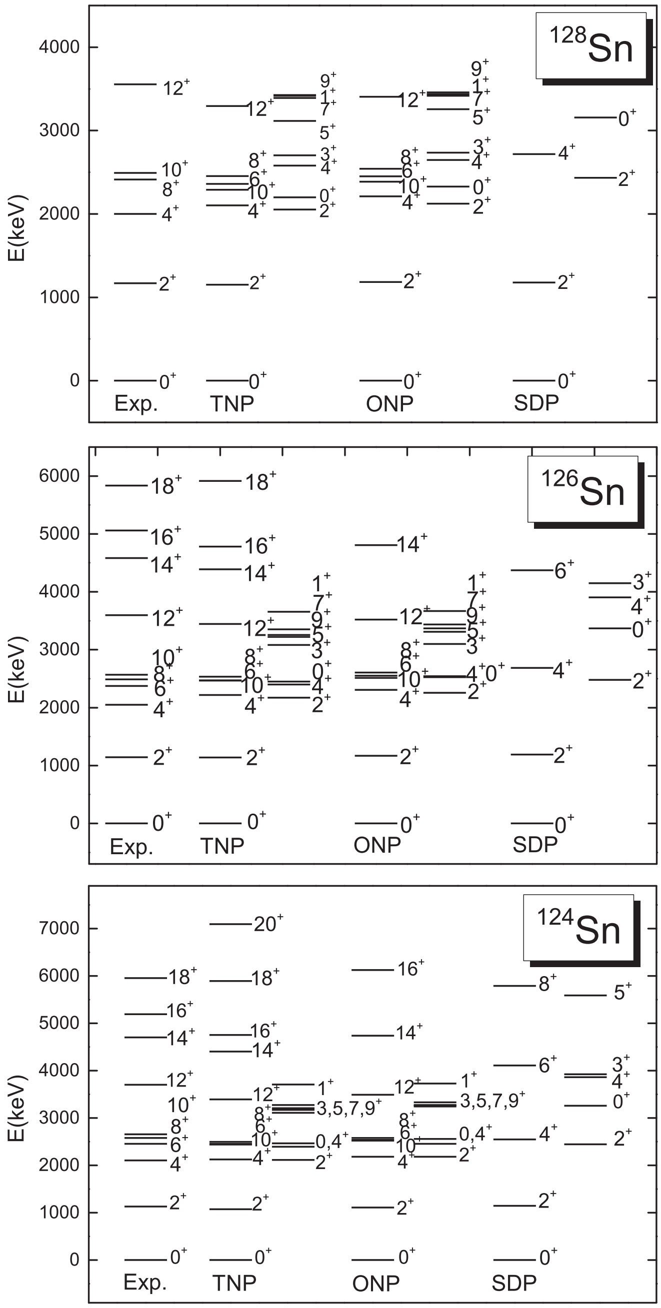

FIG. 1. The calculated spectrum for ^{128,126,124}Sn. Experimental values are taken from Refs. [28,30].

The many-pair basis is defined as

$$\begin{aligned} |\tau, J_N, M_N\rangle &= |r_1 r_2 \cdots {}_N\,; J_1 J_2 J_3 \cdots J_N\rangle = A_{M_N}^{J_N\dagger}(r_i, J_i)|0\rangle, \\ \tau &\equiv (r_1 r_2 \cdots r_N; J_1 J_2 J_3 \cdots J_{N-1}). \end{aligned} \tag{6}$$

where the number of pairs with given angular momentum or type (collective or noncollective pair) can be counted out clearly.

To study the effects of the noncollective pairs, a simple Hamiltonian composed of the monopole pairing, quadrupole pairing, and quadrupole-quadrupole interaction for like

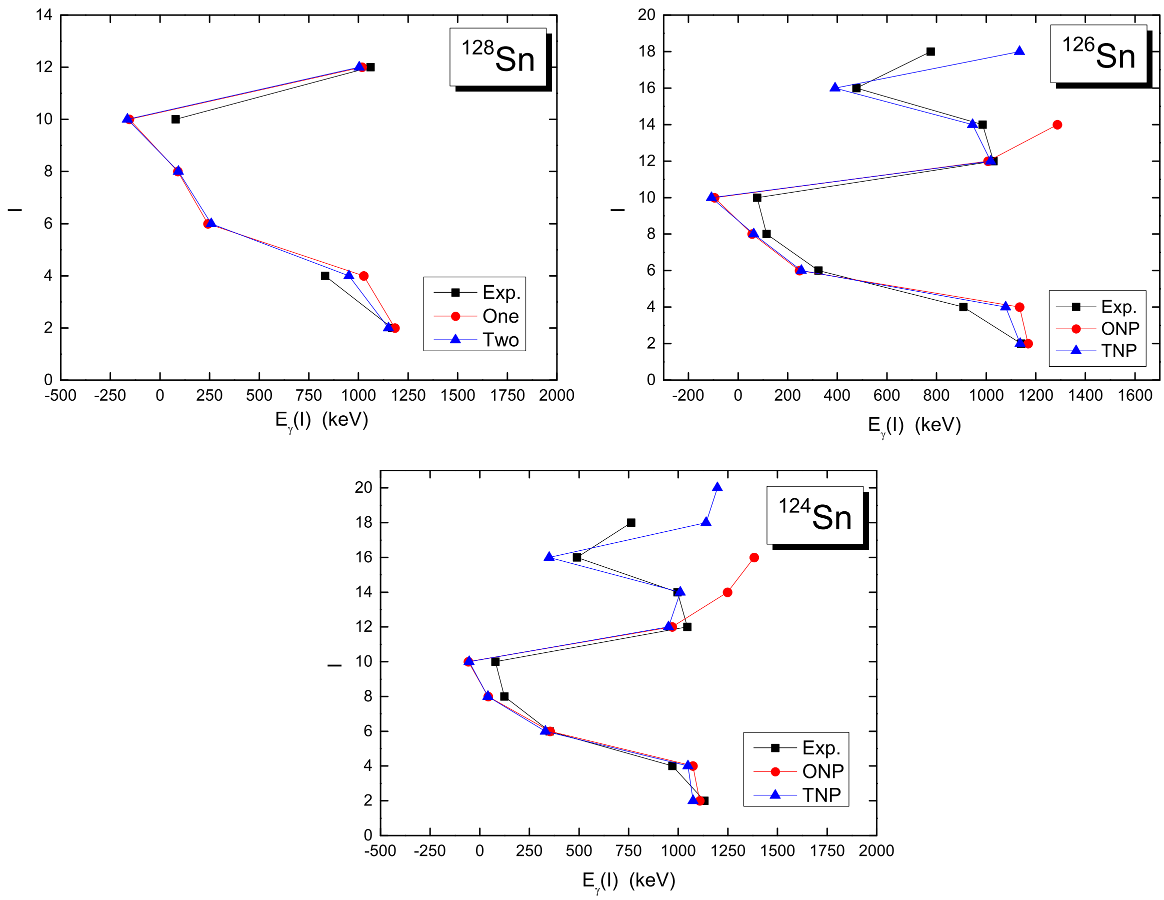

FIG. 2. γ-ray energies $E_\gamma(I)$ against the angular momentum I.

valence nucleons is adopted, which can be written as

$$\begin{aligned} H &= H_0 - G_0 P^{(0)} P^{(0)\dagger} - G_2 P^{(2)} P^{(2)\dagger} - \kappa Q^2 \cdot Q^2, \\ H_0 &= \sum_a \epsilon_a C_a^\dagger C_a, \\ P^{(0)\dagger} &= \sum_a \frac{\hat{a}}{2} (C_a^\dagger \times C_a^\dagger)^0, \\ P^{(2)\dagger} &= \sum_a q(ab2)(C_a^\dagger \times C_a^\dagger)^2, \end{aligned} \tag{7}$$

where H_0 is the single-particle energy term, and G_0, G_2, and κ are the monopole pairing, the quadrupole pairing, and the quadrupole-quadrupole interaction strength, respectively.

The $E2$ transition operator is simply given by

$$T(E2) = e_\nu Q^{(2)}, \tag{8}$$

where e_ν represents the effective charge of the valence neutron-holes, which is taken to be $e_\nu = -1.0e$ for simplicity, where the minus sign is due to the hole-type valence neutrons. More details of the model can be found in Ref. [4].

III. RESULTS AND DISCUSSIONS

To study the effect of the noncollective pairs for ^{124,126,128}Sn, three cases are considered in this paper, i.e., the case without the noncollective pairs denoted as SDP, the case with one noncollective pair denoted as ONP, and the case with two noncollective pairs denoted as TNP. The single-particle energies of the model are obtained from the first a few excited level energies with the corresponding spin and parity of nucleus $^{131}_{50}$Sn$_{81}$, which is 0.332, 0.242, 0.0, 1.655, and 2.434 MeV for the $2s_{1/2}$, $0h_{11/2}$, $1d_{3/2}$, $1d_{5/2}$, and $0g_{7/2}$ orbits, respectively, taken from Ref. [29]. By the best fit to the experimental level energies of ^{130}Sn in the collective SD-pair subspace, the model parameters with $G_0 = 0.15$ MeV, $G_2 = 0.017$ MeV$/r_0^4$, and $\kappa = 0.045$ MeV$/r_0^4$ are obtained, which will be fixed in the model calculations for ^{124,126,128}Sn in the following.

A. Spectra

The low-lying-energy spectra of ^{124,126,128}Sn calculated from the model with the SDP, ONP, and TNP cases are shown Fig. 1. As shown in Fig. 1, in the SDP case, except for the 2_1^+ level energy, which is always close to the experimental value, the other calculated level energies are all higher than the experimental ones. Furthermore, there is staggering in the 6_1^+, 8_1^+, and 10_1^+ levels; namely, these levels do not distribute as uniformly as 0_1^+, 2_1^+, 4_1^+ levels in the yrast band of the three nuclei, which, however, cannot be reproduced in the SDP case.

In the ONP case, one can see that, except for the level ordering of 6_1^+, 8_1^+, and 10_1^+, which is 10_1^+, 6_1^+, and 8_1^+ obtained from the model calculation, is different from that of the experiments [28,30], a general agreement between the

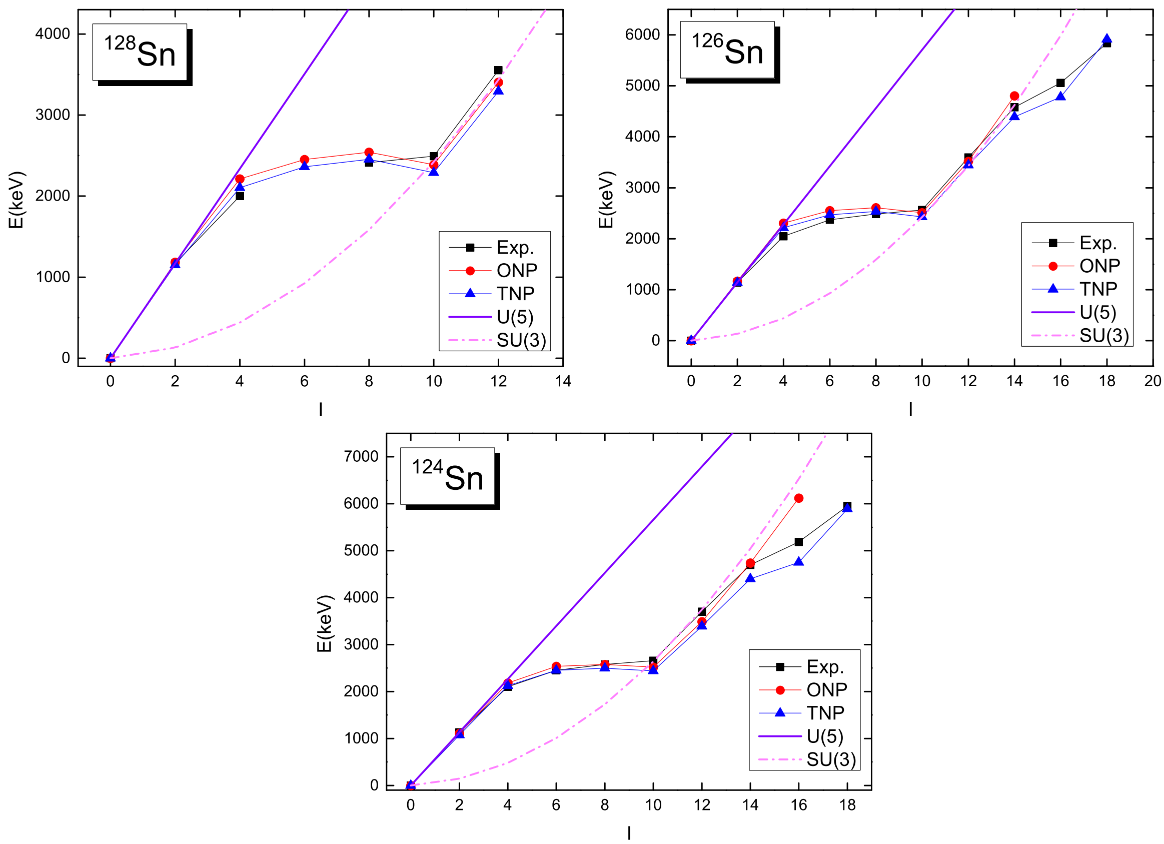

FIG. 3. Energies against angular momentum I for ^{124,126,128}Sn. The vibrational [U(5)] and rotational [SU(3)] limits are also provided for comparison.

calculated results and experimental results is achieved for the three nuclei considered. The staggering in the yrast states of the three nuclei can also be well reproduced. Moreover, one can see that the TNP results are close to the ONP results for $I \leqslant 12$. The small level spacing between 14^+ and 16^+ in ^{124,126}Sn can also be satisfactorily produced in the TNP case.

It is clearly shown from the overall fitting shown in Fig. 1 that, for ^{124,126,128}Sn, the noncollective pair should be considered in the *SD*-pair shell model, and the second noncollective pair is necessary for the higher-lying states.

From the above analysis, it is shown that the yrast states in ^{124,126,128}Sn can be fit very well in the ONP and TNP cases. Since the backbending phenomena were proposed [31] in 1971 for the first time, irregular yrast sequences have been observed in many even-even nuclei. Similar phenomena have also been observed in odd-A nucleus [32,33] and light nuclei [34]. The second backbending phenomena have also been observed [35]. Many theoretical methods have been used to study the backbending phenomena [36–41]. The mechanism of backbending is interpreted as a band-crossing between the ground band and the superband (S band), which is constructed from the alignment of two neutrons in high-j orbit [42]. To see the effects of the noncollective pairs more clearly, $E_\gamma(I) = E(I) - E(I-2)$ against the angular momentum I is presented in Fig. 2, from which one can see that the experimental results for $I \leqslant 12$ can be reproduced very well in both the ONP and TNP cases, but the second backbending phenomena can only be reproduced in the TNP case, which may imply the second noncollective pair gradually aligning in $\nu h_{11/2}$ orbit.

The yrast states of the heavy Sn isotopes are expected to be only due to excitations of neutrons moving in a spherical well, particularly due to several broken pairs in the $\nu h_{11/2}$ orbit [28]. Therefore, to reveal the effect of the noncollective pairs, the excitation energies against angular momentum I are presented in Fig. 3, in which the results in the vibrational and rotational limits [42,43] are also provided. As can be observed, our calculated results can describe the tendency of the transition from vibrational to rotational pattern satisfactorily. The distribution of 0_1^+, 2_1^+, and 4_1^+ levels of the three nuclei indicate that they are close to the vibrational pattern, i.e., the shape of the three nuclei are almost spherical in the low-lying states. Due to the small deformation caused by neutron alignment in the $\nu h_{11/2}$ orbit, the yrast line gradually approaches the rotational limit. It can also be seen that the results of $I = 16$, 18 levels in ^{124,126}Sn can also be reproduced by including the second noncollective pair.

In Ref. [44], a simple method, E-gamma over spin (E-GOS), has been used to discern the level pattern evolution from the vibrational to the rotational type. In this method, the microscopic explanation of the backbending and the shape phase transition are due to the alignment of nucleons in a high-j orbit. Many nuclei with similar properties have been studied with this method [45–47]. To see if the SDPSM can reproduce the level pattern evolution from the vibrational to the rotational type more clearly, the E-GOS plots for these

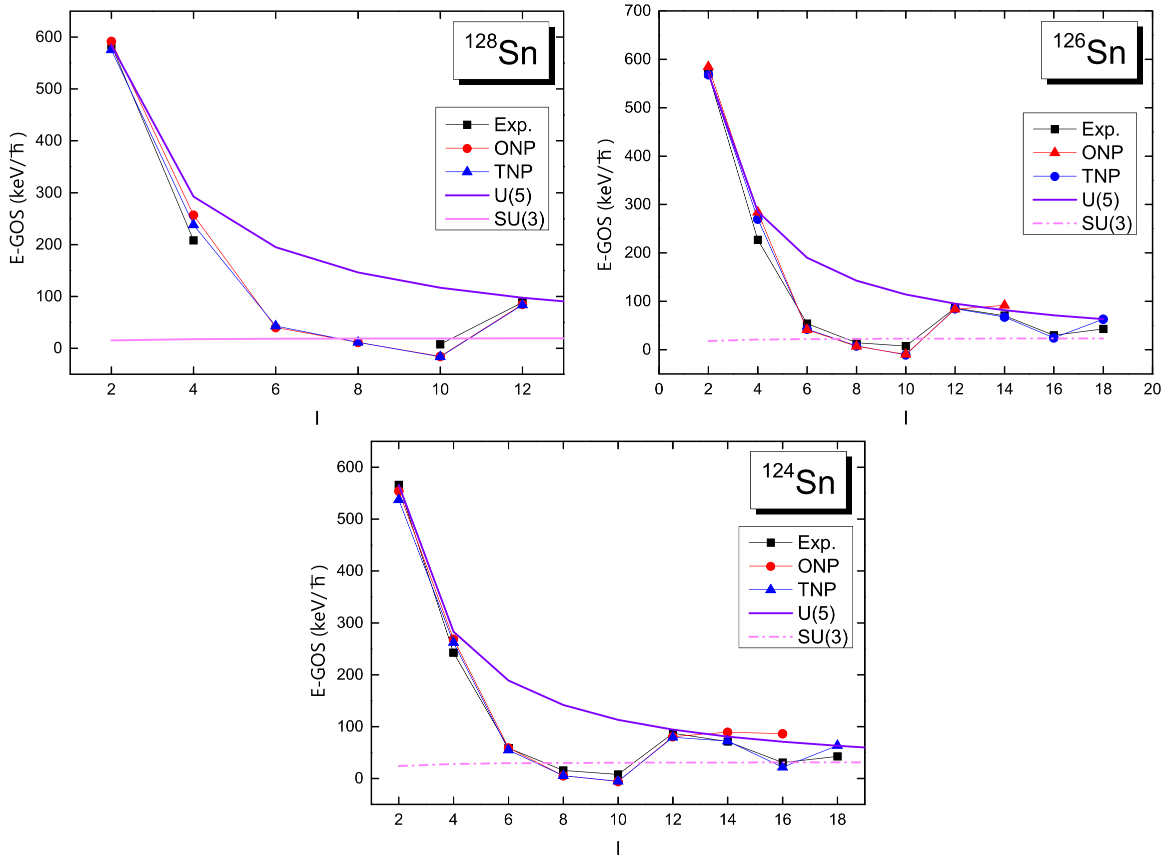

FIG. 4. The E-GOS (keV/$\hbar$) vs angular momentum plot. The vibrational [U(5)] and rotational [SU(3)] limit results are also presented.

three nuclei are shown in Fig. 4, from which one can clearly see the level pattern evolution from vibrational to rotational type [44] described by the model results, which track the experimental data very well. One may also notice that the experimental results can be described very well up to $I = 14$ in both the ONP and TNP cases, but for the levels with $I = 16$ and $I = 18$, the experimental results can only be fit in the TNP case, i.e., the second noncollective pair is needed.

B. $B(E2)$ ratios

To further reveal the effect of the noncollective pairs, the calculated $B(E2)$ ratios $[B(E2, I \rightarrow I-2)/B(E2, 2 \rightarrow 0)]$ of ^{124,126,128}Sn along the yrast states are presented in Fig. 5, in which the results calculated in the shell model, the pair truncated shell model (PTSM) [25], and some available experimental values are also shown. It is shown from Fig. 5 that, for ^{128}Sn, the available experimental values can be fit very well in the shell model and the in PTSM. The results obtained from the ONP and TNP cases are close to each other, which are slightly larger than the corresponding experimental values. Figure 5 also shows that the behavior of the $B(E2)$ ratios in the shell model, the PTSM, the ONP, and the TNP cases are similar to one another for ^{128}Sn.

For ^{126}Sn, one can see that the available experimental values can be produced satisfactorily in all these four cases. The $B(E2)$ ratios in the shell model and PTSM are close to each other. The $B(E2)$ ratios calculated in the ONP and TNP cases are also close to each other. One can also see that the ONP and TNP results are different from those of the shell model and PTSM for $I = 8$ and $I \leqslant 14$.

For ^{124}Sn, the experimental value for $I = 4$ cannot be produced satisfactorily in all the four cases, i.e., the results in shell model, ONP, and TNP are all larger than the experimental one, but that of the PTSM is smaller than the experimental one. While the experimental value for $I = 10$ can be fit very well in the four cases. It is also seen that the results in ONP and TNP cases are still close to each other when $I \leqslant 14$. Except for $I = 8,\ 14$, our results are close to the shell-model results, while the results in the PTSM are all smaller than the other three cases. One can also see that, for $I = 16$, the result in the TNP case is close to that of the shell model, which may suggest that the second noncollective pair is necessary for higher-lying states.

From the above analysis, one can see that, without adjusted parameters for the three nuclei, the experimental $B(E2)$ ratios can be fit approximately. The $B(E2)$ ratios obtained in the ONP and TNP cases are close to each other for $I \leqslant 12$. Due to the lack of the experimental data, it is hard to determine the effect of the second noncollective pair to the $B(E2)$ ratios for the states with $I \geqslant 14$ in the SDPSM.

C. Occupation number of noncollective pairs

To further reveal the effects of the noncollective pairs, the occupation number of the noncollective pairs in the yrast

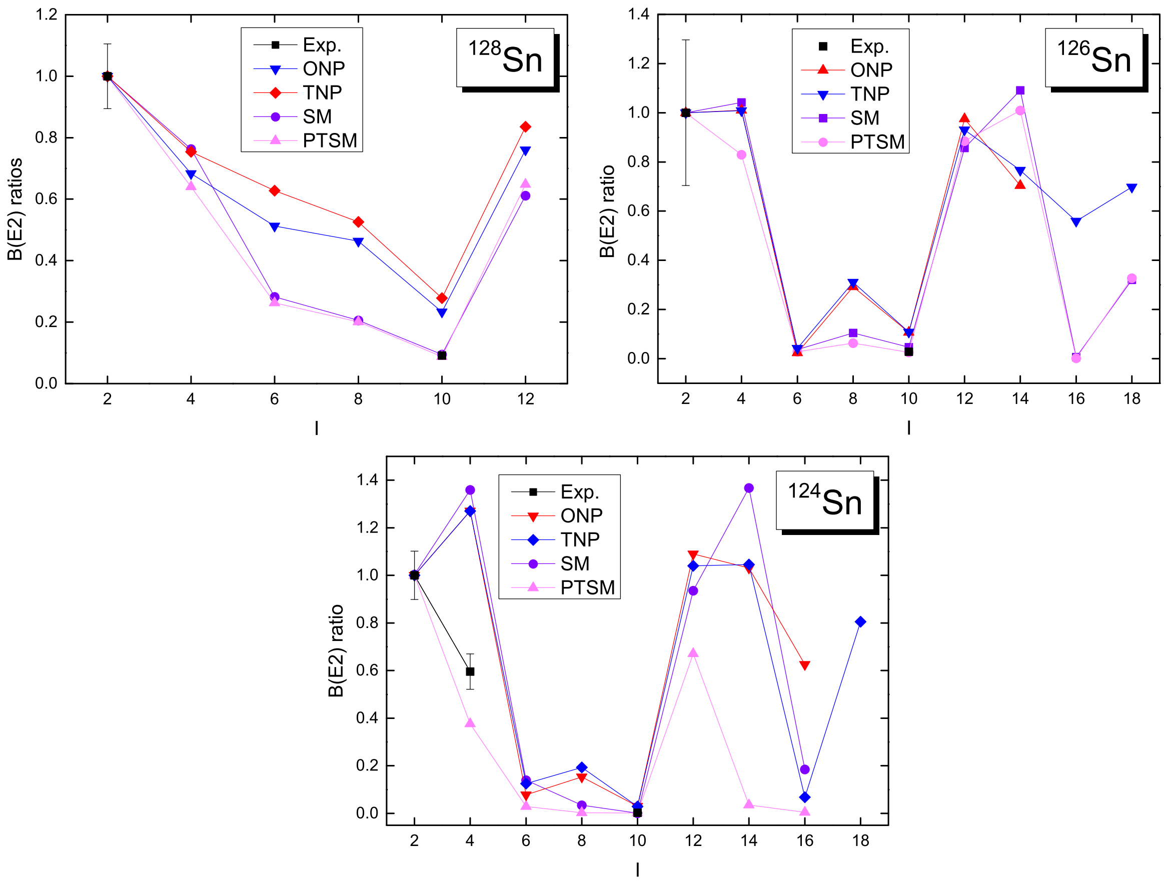

FIG. 5. $B(E2)$ ratios, $B(E2, I \rightarrow I-2)/B(E2, 2 \rightarrow 0)$, against spin I. The PTSM results and the shell-model calculations are taken from Ref. [25]. Experimental data are taken from Refs. [21,22,48–51].

states of ^{128,126,124}Sn is calculated. First, the occupation number of the noncollective pairs in each state with spin I is calculated, with the results given in Fig. 6. It is seen that the occupation number of noncollective pairs in the 0_1^+ states is close to zero for the three nuclei, i.e., the ground states are pure collective states for the three nuclei. The 2_1^+ states for the three nuclei can still be considered collective states since the occupation numbers of the noncollective pairs are all smaller than 0.2. For the states with $4 \leqslant I \leqslant 12$, the occupation number of the noncollective pairs in each state approaches 1, which implies that these states are all a mixture of the collective degrees of freedom with the noncollective degrees of freedom. For the states with $I \geqslant 14$, the occupation number of the noncollective pairs in the TNP case increases, which suggests that the second noncollective pair begin to play important role for the second backbending, as shown in Fig. 2. Figure 6 also shows that the occupation number of the noncollective pairs in each state obtained from the ONP and TNP cases is almost the same for $I \leqslant 12$.

To see the structure of the excited states more clearly, the occupation number of noncollective pairs with definite angular momentum for a given state with spin I is also calculated. The results of the ONP and TNP cases for ^{124}Sn are presented in Fig. 7, in which the occupation number of the noncollective pairs with angular momentum 0, 2, 4, 6, 8, and 10 are denoted S, D, G, I, K, and M, respectively. From Fig. 7(a), it is seen that the occupation number of the S pair is about 0.1 for the 0_1^+, and it is zero for the other states, i.e., the S pair does not contribute to the excited states in the ONP case; the occupation number of the D pair is about 0.05 and 0.2 for the 2_1^+ and 4_1^+ states, respectively; the occupation number of the G pairs is about 0.4 for the 4_1^+ state; the occupation number of the I or K pairs is about 1.0 for both the 6_1^+ and 8_1^+ states. From $I \geqslant 10$, the occupation number of the M pairs is about 1.0, which implies that two neutrons gradually align in the $\nu h_{11/2}$ orbit with increasing I. Similar results can also been found in the explanation of the backbending phenomena in Refs. [11,12].

Figure 7(b) shows that the distributions of the S, D, G, I, K, and M pairs in each state are similar to those in the ONP case for the states with $I \leqslant 12$, but for the state with $I \geqslant 14$, the second noncollective pair in the $\nu h_{11/2}$ orbit begins to align and play an important role for higher-lying states. The occupation number of the noncollective pairs for state with $I = 14$ is about 1.6 in total, and it is about 2.0 for the states with $I = 16$ and $I = 18$.

IV. SUMMARY AND DISCUSSIONS

In this work, the effects of the noncollective pairs are analyzed in the SD-pair shell-model framework. ^{128,126,124}Sn are investigated as examples with at most two noncollective

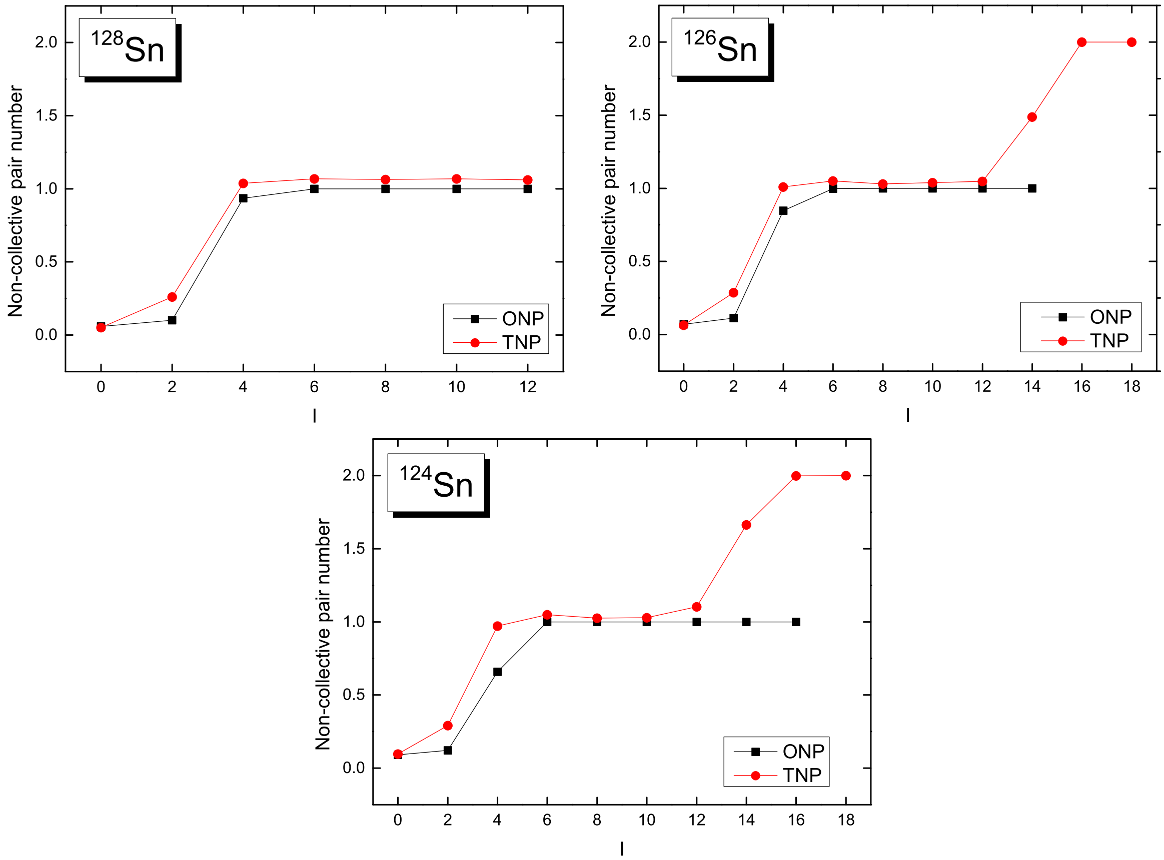

FIG. 6. Number of noncollective pairs calculated from the ONP and TNP cases.

pairs originating from neutron alignment in the $\nu h_{11/2}$ orbit. It is found that, by introducing the noncollective pairs, the yrast levels can be fit satisfactorily, and the backbending and the shape phase transition from vibration to the rotation in the yrast levels can also be described very well in the case with one noncollective pair or two noncollective pairs. The second backbending can even be well fit in the case with two noncollective pairs. From the analysis of the occupation number of the noncollective pairs in excited states, it is found that the mechanism of the backbending or the shape phase transition is the band crossing between the ground band and S band or the neutron alignment. It is also found that, for higher-lying states, the second noncollective pair begin to align in the $\nu h_{11/2}$ orbit, which seems necessary in order to reproduce the second backbending in the yrast band.

From Ref. [52] it is known that the results obtained in the exact shell model (SM) can be reproduced in the SDPSM.

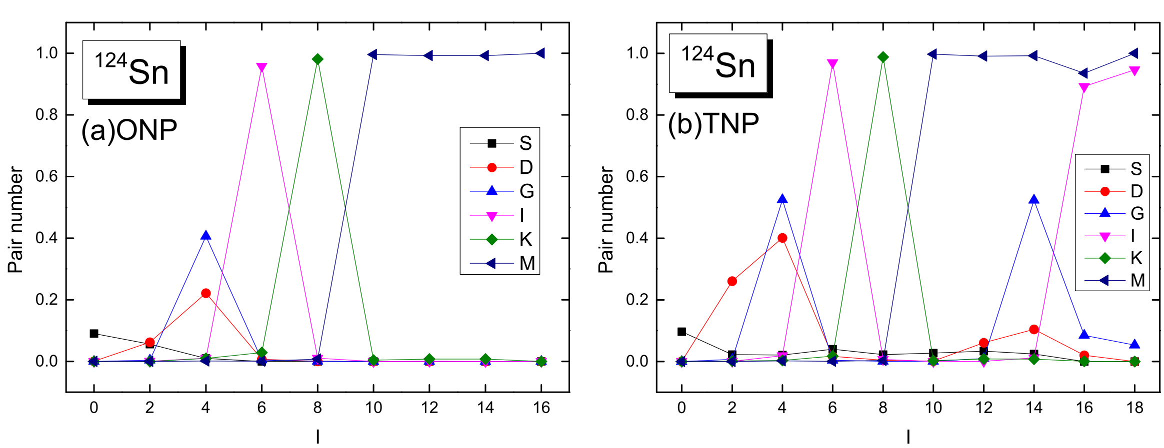

FIG. 7. Number of noncollective pairs with definite angular momentum.

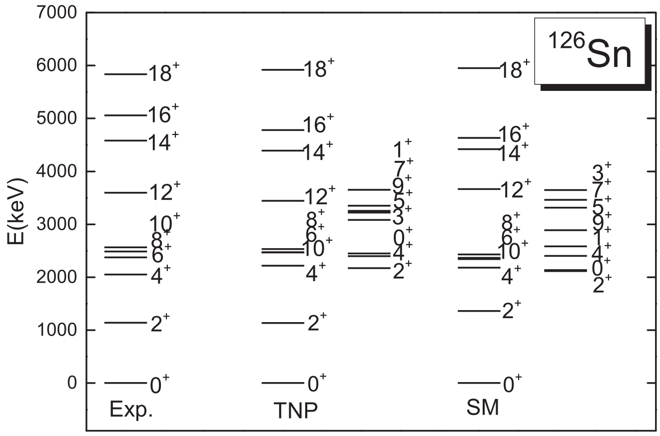

FIG. 8. The calculated spectrum for ^{126}Sn, where SM represents for the results we got in the exact shell-model case. Experimental values are taken from Refs. [28,30].

It is interesting to see if the results we report in this paper can be produced in the SM. To this end, the properties of the three-nuclei ^{128,126,124}Sn are studied with the OSLO-FCI code [53]. The Hamiltonian and the parameters used in the SM are same as those in the SDPSM. As an example, the calculated results for ^{126}Sn are presented in Fig. 8, from which one can see that the SM results are close to those of the TNP and experiments. These results may suggest that the conclusion we have drawn in this work has a solid shell-model foundation and the backbending phenomenon is rooted in the noncollective pair or the neutron alignment in the $h_{11/2}$ orbit.

ACKNOWLEDGMENTS

This work was supported by the Natural Science Foundation of China (Grants No. 11475091, No. 11875171, No. 11675071, and No. 11875158).

[1] J.-Q. Chen, Nucl. Phys. A **562**, 218 (1993).
[2] J.-Q. Chen, B.-Q. Chen, and K. Abraham, Nucl. Phys. A **554**, 61 (1993).
[3] Y. Zhao and A. Arima, Phys. Rep. **545**, 1 (2014).
[4] J.-Q. Chen, Nucl. Phys. A **626**, 686 (1997).
[5] Y.-A. Luo, J.-Q. Chen, and J. Draayer, Nucl. Phys. A **669**, 101 (2000).
[6] G. J. Fu, Y. Lei, Y. M. Zhao, S. Pittel, and A. Arima, Phys. Rev. C **87**, 044310 (2013).
[7] Y.-A. Luo, F. Pan, C. Bahri, and J. P. Draayer, Phys. Rev. C **71**, 044304 (2005).
[8] L. Li, Y. A. Luo, T. Wang, F. Pan, and J. P. Draayer, J. Phys. G **36**, 125107 (2009).
[9] Y.-A. Luo, F. Pan, T. Wang, P.-z. Ning, and J. P. Draayer, Phys. Rev. C **73**, 044323 (2006).
[10] Y.-A. Luo, Y. Zhang, X. Meng, F. Pan, and J. P. Draayer, Phys. Rev. C **80**, 014311 (2009).
[11] K. Higashiyama, N. Yoshinaga, and K. Tanabe, Phys. Rev. C **67**, 044305 (2003).
[12] T. Takahashi, N. Yoshinaga, and K. Higashiyama, Phys. Rev. C **71**, 014305 (2005).
[13] A. Banu, J. Gerl, C. Fahlander, M. Górska, H. Grawe, T. R. Saito, H. J. Wollersheim, E. Caurier, T. Engeland, A. Gniady, M. Hjorth-Jensen, F. Nowacki, T. Beck, F. Becker, P. Bednarczyk, M. A. Bentley, A. Bürger, F. Cristancho, G. de Angelis, Zs. Dombrádi, P. Doornenbal, H. Geissel, J. Grebosz, G. Hammond, M. Hellström, J. Jolie, I. Kojouharov, N. Kurz, R. Lozeva, S. Mandal, N. Mărginean, S. Muralithar, J. Nyberg, J. Pochodzalla, W. Prokopowicz, P. Reiter, D. Rudolph, C. Rusu, N. Saito, H. Schaffner, D. Sohler, H. Weick, C. Wheldon, and M. Winkler, Phys. Rev. C **72**, 061305(R) (2005).
[14] J. Cederkäll, A. Ekström, C. Fahlander, A. M. Hurst, M. Hjorth-Jensen, F. Ames, A. Banu, P. A. Butler, T. Davinson, U. Datta Pramanik, J. Eberth, S. Franchoo, G. Georgiev, M. Górska, D. Habs, M. Huyse, O. Ivanov, J. Iwanicki, O. Kester, U. Koster, B. A. Marsh, O. Niedermaier, T. Nilsson, P. Reiter, H. Scheit, D. Schwalm, T. Sieber, G. Sletten, I. Stefanescu, J. Van de Walle, P. van Duppen, N. Warr, D. Weisshaar, and F. Wenander, Phys. Rev. Lett. **98**, 172501 (2007).
[15] C. Vaman, C. Andreoiu, D. Bazin, A. Becerril, B. A. Brown, C. M. Campbell, A. Chester, J. M. Cook, D. C. Dinca, A. Gade *et al.*, Phys. Rev. Lett. **99**, 162501 (2007).
[16] A. Ekström, J. Cederkäll, C. Fahlander, M. Hjorth-Jensen, F. Ames, P. A. Butler, T. Davinson, J. Eberth, F. Fincke, A. Görgen *et al.*, Phys. Rev. Lett. **101**, 012502 (2008).
[17] P. Doornenbal, P. Reiter, H. Grawe, H. J. Wollersheim, P. Bednarczyk, L. Caceres, J. Cederkäll, A. Ekström, J. Gerl, M. Górska, A. Jhingan, I. Kojouharov, R. Kumar, W. Prokopowicz, H. Schaffner, and R. P. Singh, Phys. Rev. C **78**, 031303(R) (2008).
[18] G. Guastalla, D. D. DiJulio, M. Górska, J. Cederkäll, P. Boutachkov, P. Golubev, S. Pietri, H. Grawe, F. Nowacki, K. Sieja *et al.*, Phys. Rev. Lett. **110**, 172501 (2013).
[19] P. Doornenbal, S. Takeuchi, N. Aoi, M. Matsushita, A. Obertelli, D. Steppenbeck, H. Wang, L. Audirac, H. Baba, P. Bednarczyk, S. Boissinot, M. Ciemala, A. Corsi, T. Furumoto, T. Isobe, A. Jungclaus, V. Lapoux, J. Lee, K. Matsui, T. Motobayashi, D. Nishimura, S. Ota, E. C. Pollacco, H. Sakurai, C. Santamaria, Y. Shiga, D. Sohler, and R. Taniuchi, Phys. Rev. C **90**, 061302(R) (2014).
[20] L. Coraggio, A. Covello, A. Gargano, N. Itaco, and T. T. S. Kuo, Phys. Rev. C **91**, 041301(R) (2015).
[21] C. T. Zhang, P. Bhattacharyya, P. J. Daly, Z. W. Grabowski, R. Broda, B. Fornal, and J. Blomqvist, Phys. Rev. C **62**, 057305 (2000).
[22] R. Broda, R. H. Mayer, I. G. Bearden, P. Benet, P. J. Daly, Z. W. Grabowski, M. P. Carpenter, R. V. F. Janssens, T. L. Khoo, T. Lauritsen *et al.*, Phys. Rev. Lett. **68**, 1671 (1992).
[23] J. Walker, A. Jungclaus, J. Leske, K.-H. Speidel, A. Ekström, P. Boutachkov, J. Cederkäll, P. Doornenbal, J. Gerl, R. Gernhäuser *et al.*, Phys. Rev. C **84**, 014319 (2011).
[24] M. P. Kartamyshev, T. Engeland, M. Hjorth-Jensen, and E. Osnes, Phys. Rev. C **76**, 024313 (2007).
[25] Y. Y. Cheng, C. Qi, Y. M. Zhao, and A. Arima, Phys. Rev. C **94**, 024321 (2016).
[26] Y. Y. Cheng, Y. M. Zhao, and A. Arima, Phys. Rev. C **97**, 024303 (2018).
[27] L. Y. Jia and C. Qi, Phys. Rev. C **94**, 044312 (2016).

[28] A. Astier, M.-G. Porquet, C. Theisen, D. Verney, I. Deloncle, M. Houry, R. Lucas, F. Azaiez, G. Barreau, D. Curien *et al.*, Phys. Rev. C **85**, 054316 (2012).
[29] B. Fogelberg and J. Blomqvist, Nucl. Phys. A **429**, 205 (1984).
[30] S. Pietri, A. Jungclaus, M. Górska, H. Grawe, M. Pfützner, L. Cáceres, P. Detistov, S. Lalkovski, V. Modamio, Z. Podolyák *et al.*, Phys. Rev. C **83**, 044328 (2011).
[31] A. Johnson, H. Ryde, and J. Sztarkier, Phys. Lett. B **34**, 605 (1971).
[32] E. Grosse, F. S. Stephens, and R. M. Diamond, Phys. Rev. Lett. **31**, 840 (1973).
[33] E. Grosse, F. S. Stephens, and R. M. Diamond, Phys. Rev. Lett. **32**, 74 (1974).
[34] E. M. Szanto, A. Szanto de Toledo, H. V. Klapdor, M. Diebel, J. Fleckner, and U. Mosel, Phys. Rev. Lett. **42**, 622 (1979).
[35] I. Y. Lee, M. M. Aleonard, M. A. Deleplanque, Y. El-Masri, J. O. Newton, R. S. Simon, R. M. Diamond, and F. S. Stephens, Phys. Rev. Lett. **38**, 1454 (1977).
[36] G. Martínez-Pinedo, A. Poves, L. M. Robledo, E. Caurier, F. Nowacki, J. Retamosa, and A. Zuker, Phys. Rev. C **54**, R2150(R) (1996).
[37] K. Hara, Y. Sun, and T. Mizusaki, Phys. Rev. Lett. **83**, 1922 (1999).
[38] A. Faessler, M. Ploszajczak, and K. Devi, Nucl. Phys. A **301**, 382 (1978).
[39] R. Bengtsson, I. Hamamoto, and B. Mottelson, Phys. Lett. B **73**, 259 (1978).
[40] C. J. Pearson, P. M. Walker, C. S. Purry, G. D. Dracoulis, S. Bayer, A. P. Byrne, T. Kibédi, F. G. Kondev, T. Shizuma, R. A. Bark *et al.*, Phys. Rev. Lett. **79**, 605 (1997).
[41] R. A. Herrera and C. W. Johnson, Phys. Rev. C **95**, 024303 (2017).
[42] P. Ring, *The Nuclear Many-Body Problem* (Springer-Verlag, Berlin, Heidelberg, 1980).
[43] F. Iachello and A. Arima, *The Interacting Boson Model* (Cambridge University Press, Cambridge, England, 1987).
[44] P. H. Regan, C. W. Beausang, N. V. Zamfir, R. F. Casten, J. Y. Zhang, A. D. Yamamoto, M. A. Caprio, G. Gürdal, A. A. Hecht, C. Hutter, R. Krücken, S. D. Langdown, D. A. Meyer, and J. J. Ressler, Phys. Rev. Lett. **90**, 152502 (2003).
[45] K. Heyde, J. Jolie, R. Fossion, S. De Baerdemacker, and V. Hellemans, Phys. Rev. C **69**, 054304 (2004).
[46] P. Cejnar and J. Jolie, Phys. Rev. C **69**, 011301(R) (2004).
[47] Y.-X. Liu, L.-Z. Mu, and H. Wei, Phys. Lett. B **633**, 49 (2006).
[48] J. M. Allmond, A. E. Stuchbery, D. C. Radford, A. Galindo-Uribarri, N. J. Stone, C. Baktash, J. C. Batchelder, C. R. Bingham, M. Danchev, C. J. Gross *et al.*, Phys. Rev. C **87**, 054325 (2013).
[49] B. Fogelberg, K. Heyde, and J. Sau, Nucl. Phys. A **352**, 157 (1981).
[50] D. Radford, C. Baktash, J. Beene, B. Fuentes, A. Galindo-Uribarri, J. G. del Campo, C. Gross, M. Halbert, Y. Larochelle, T. Lewis *et al.*, Nucl. Phys. A **746**, 83 (2004).
[51] www.nndc.bnl.gov/ensdf
[52] Y. M. Zhao, N. Yoshinaga, S. Yamaji, and A. Arima, Phys. Rev. C **62**, 014316 (2000).
[53] T. Engeland and M. Hjorth-Jensen, The Oslo-FCI Code, https://github.com/ManyBodyPhysics/ManybodyCodes/